A Passive Front End of Radio Transceivers for LTE Bands

Marwa Mansour
Ain shams university
Cairo – Egypt

Abdelhalim Zekry
Ain shams university
Cairo – Egypt

R.S. Ghoname
Faculty of Engineering
Girls'Campus
King Abdulaziz university
,Jeddah Saudia Arabia(1)
Electronics Research Institute,
Cairo, Egypt

ABSTRACT
Software defined radio implementation is required for LTE radio transceivers. An SDR consists of an rf front end and a digital processor platform DSP. This paper is devoted to the design and implementation of the passive part of the front end; the antennas and bandpass filters. It presents the design of two microstrip patch antennas and a third order parallel coupled band pass filter with defected ground structure that can be used in cellular communication applications, especially in LTE . The two antennas cover LTE network bands 1, 2, 3, 4, 9, 10, 23, 25, 33, 34, 35, 36, 37, and 39[1]. The antennas and filter were printed using FR-4 substrate material with dielectric constant of ε_r =4.4, thickness of h = 1.6 mm and loss tangent tan δ = 0.025.

The overall dimensions of the first antenna is 39 mm * 37mm * 1.6 mm with 50 Ω impedance. This antenna operates between 1666 MHz and 2239.5MHz for return loss of less than - 6 dB and covers LTE network bands 1, 2, 3, 4, 9, 10, 23, 25, 33, 34, 35, 36, 37, and 39. The simulation results suggest that the antenna gain and directivity value are 1.7dB and 2.5 dBi with omnidirectional radiation pattern.

The overall dimension of the second antenna is 25 mm * 21mm * 1.6 mm with 50 Ω impedance. This antenna operates between 1896MHz and 2015.8MHz for return loss of less than - 6dB and covers LTE network bands 1, 2, 25, 33, 36, and 37. The simulation results suggest that the antenna gain and directivity value are 1.4dB and 1.7dBi with omnidirectional radiation pattern.

The parallel coupled filter with over all dimensions of 45 mm * 25 mm achieves centers frequency of 1.95 GHz and band width of 80 MHz and covers LTE network bands 36 or 1. The order of the proposed band pass filter is three and three defected ground structure are used.

The devices are analyzed using Computer Simulation technology (CST) and Zeland IE3D. They are fabricated with photolithographic techniques and their scattering parameters are measured by using Vector Network Analyzer (VNA) E8719A. Measurements and simulations show good agreement.

Keywords
LTE, Microstrip patch antenna, slit element, omnidirectional, Directivity, Gain, BPF, parallel couple band pass filter, DGS, CST, and Zeland IE3D.

1. INTRODUCTION
Long Term Evolution, LTE, marketed as 4G LTE, is a standard for wireless communication of high-speed data for mobile phones and data terminals. It refers to ongoing process of improving wireless technology so that operators can upgrade it to support existing infrastructure. It mainly aims at high data rate, low latency and improved mobility. For increased data rate LTE uses MIMO technique with multiple antennas at transmitter and receiver. LTE operates over different frequencies in the range from 400MHz to 4GHz licensed frequency bands [1].

In this paper it is required to design and implement the rf passive front end of an LTE wireless transceivers covering the bands 1(FDD) or 36 (TDD). One of the most appropriate technologies in the frequency range is the microstrip circuits. The passive front end comprises an antenna and a bandpass filter. The most proper antenna shape is the patch antennas[2].

Patch antenna consists of a metallic patch on one side of a dielectric substrate. The value of the relative permeability (ε_r) depends on the materials which can be copper, silver, gold, aluminum. A substrate FR4 epoxy with a dielectric constant in the range $2.2 \leq \varepsilon_r \leq 12$ is used [3]. The patch can be rectangular, circular, elliptical, triangular or any other shape. For a rectangular patch, the length L of the element is usually $\lambda o/3 < L < \lambda o/2$. The length, height and width of the patch and its substrate are given by standard formulas [2]. The patch can be feed by means of a number of techniques that are Microstrip transmission-line feed, Aperture coupling feed, Coaxial probe feed and Proximity coupling feed [4].

A band pass filter is an important component that must be added after or before the antenna to reject the out of band signals in the rf receivers and transmitters, respectively. It is a passive component which is able to select signals inside a specific bandwidth at a certain center frequency and reject signals in another frequency region, especially in frequency regions, which have the potential to interfere the information signals.

In designing the band pass filter, we are faced with the questions, what is the maximal loss inside the pass region, and the minimal attenuation in the reject/stop regions, and how the filter characteristics must look like in transition regions [5].

In this range of frequencies, microstrip line is a good candidate for filter design due to its advantages of low cost, compact size, light weight, planar structure and easy integration with other components on a single board. To achieve better performance for the microwave filters, such as increasing steepness of the cut-off slope, and to increase the stopband range of the microwave filters, and reduce the filter size, defected ground structures (DGS) are used [6]. This technique is realized by etching slots in the ground plane of the microwave circuit. This technique is used for microstrip and coplanar waveguide transmission lines [7].

This paper is organized as follows: Details of the antenna design and resonance principle are described in Section 2. A

fabricated prototype of the antenna will be experimentally tested and analyzed in Section 3. Design of parallel coupled band pass filter is illustrated in section 4. Implementation and measurement of DGS BPF is presented in Section 5. Lastly, section 6 is the paper conclusion.

2. ANTENNA DESIGN

For rectangular patch, the width W and the length L are given in terms of the speed of light c, the resonance frequency f_o and substrate parameters as [2],

$$W = \frac{c}{2 f_o \sqrt{\frac{\epsilon_r+1}{2}}} \quad (1)$$

Eq. 2 is used to calculate the effective length of the rectangular patch,

$$L = \frac{c}{2f_o\sqrt{\epsilon eff}} - 2\Delta L \quad (2)$$

$$\text{With } \Delta L = 0.412h \frac{\epsilon eff+3(\frac{W}{h}+0.264)}{\epsilon eff-0.258(\frac{W}{h}+0.8)} \quad (3)$$

The value of the effective dielectric constant ε_{eff} is given [8] by,

$$\varepsilon_{eff} = \frac{\epsilon r+1}{2} + \frac{\epsilon r-1}{2}(1+12\frac{h}{w})^{\frac{1}{2}} \quad (4)$$

In the above formulas, h is the height of the dielectric substrate, ε_r is the relative dielectric constant for the substrate and ε_{eff} is the effective dielectric constant. Eq. 5 is used to calculate the length of the radiating patch [9],

$$L_{eff} = L + 2\Delta L \quad (5)$$

For our microtrip circuits in this paper, FR4 PCB board is used as a substrate having a thickness of h=1.6 mm, a relative permittivity ε_r =4.4 and tan δ = 0.025.

The first device to be designed is a conventional microstrip line feed rectangular patch antenna with the geometry shown in Fig. 1. The dimensions of the conventional patch are determined from above formulas assuming a resonance frequency of 1.95 GHz in the band of LTE and Z_o= 50 Ohm. The obtained dimensions are given in Table 1. In order to evaluate the performance of such antenna its reflection coefficient S11 is numerically calculated and plotted in Fig 2.

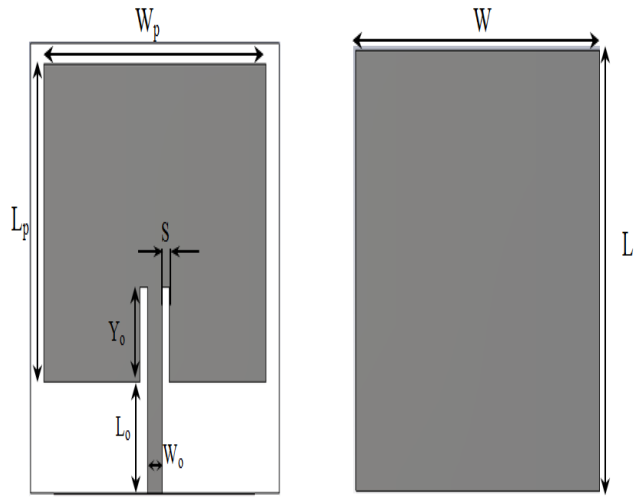

(a) (b)

Fig 1: The geometry of the conventional patch antenna. (a) Top view (b) Bottom view.

Table 1: Conventional patch geometrical parameters.

parameter	Value (mm)	parameter	Value (mm)
L	49.55	W_o	2.86
W	49.8	Y_o	10.49
L_P	35.1	L_o	12.24
W_P	44.4	S	1.5

By inspecting the results, it is clear that the antenna consumes relatively large area which means it is bulky. Its bandwidth is relatively small. So, other antenna designs are proposed to enhance this conventional type.

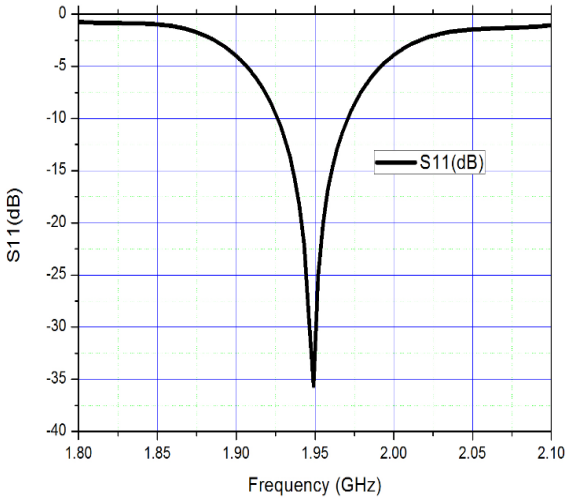

Fig 2: The simulation result for the rectangular patch antenna.

2.1 Patch Antenna with Slit and DGS

The geometry of the first proposed antenna is shown in Fig 3 and its photograph is shown in Fig 4. It is rectangular patch with a slit Ls and large defected ground structure .The antenna was designed on FR4 epoxy substrate with the overall dimension of 39 * 37.5 mm2. By adding a narrow slit close to the radiating edges the operating frequency can be varied. The ground plane has been modified by reducing its length to 3 mm to increase the bandwidth and reduce the antenna dimensions.

Table 2 shows the design values of the first antenna geometrical parameters.

The resonant frequency shift depends on the position of the Slit on the patch as shown in Fig 5:

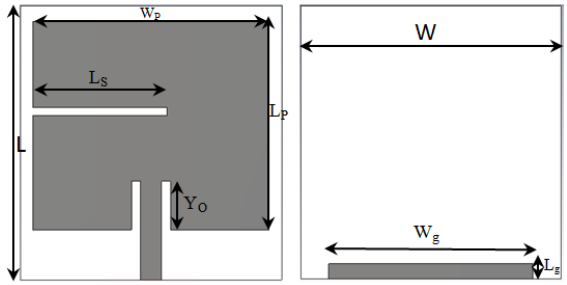

(a) (b)

Fig 3: The geometry of the first proposed antenna. (a) Top view (b) Bottom view.

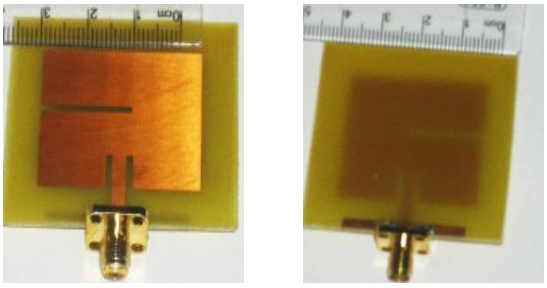

(a) (b)

Fig 4: A photo of fabricated first proposed antenna using DGS. (a) Top view. (b) Bottom view.

Table2: First Antenna Geometrical Parameters

Parameter	Value (mm)	parameter	Value (mm)
W	37.5	L_S	19.24
L	39.3	Y_o	6.97
W_P	33.93	L_g	3
L_P	29.83	W_g	29.5

The simulation results shown in Fig 5 depicts that both the resonance frequency and the bandwidth can be varied in an appreciable frequency range together with antenna bandwidth. The DGS really reduced the size of the patch and made it more compact.

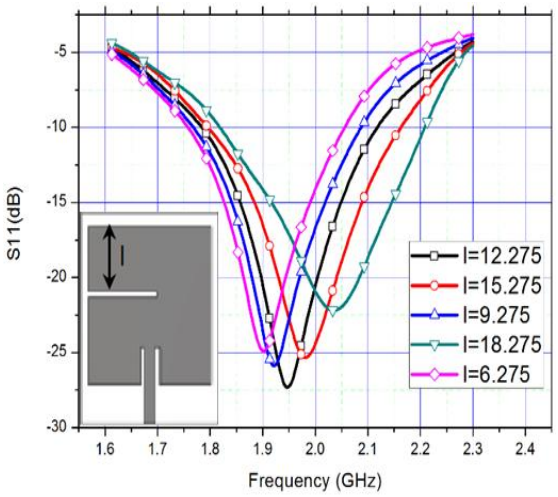

Fig 5: The effect of patch slit on the resonant frequency.

2.2 Patch Antenna with Large Slit and DGS

The configuration of the second proposed antenna is illustrated in Fig. 6. The antenna was designed on FR4 epoxy substrate with the overall dimension of 21*25 mm2, the antenna consists of rectangular patch with microstrip line feed. To decrease the antenna size further a wide slit close to the radiating edges of the patch is added together with large ground plane degeneration. So, the major geometrical difference with the first propped antenna is the large size of the slit. A photograph of the fabricated pecimen is shown in Fig 7.

Table 3 shows the design values of the second proposed antenna geometrical parameters.

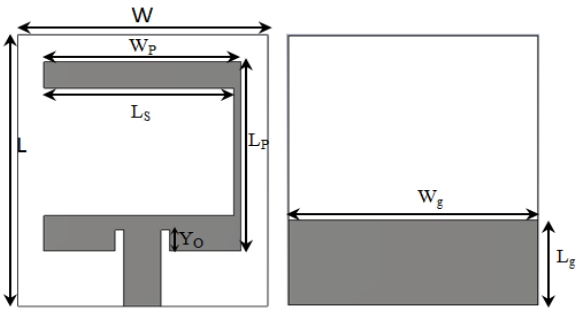

(a) (b)

Fig 6: The geometry of the second proposed antenna. (a) Top view (b) Bottom view.

(a) (b)

Fig 7: A photo of fabricated second proposed antenna using DGS. (a) Top view. (b) Bottom view.

Table 3: Second Antenna Geometrical Parameters

parameter	Value (mm)	parameter	Value (mm)
W	21	L_S	16.27
L	25	Y_o	1.97
W_P	16.73	L_g	8.101
L_P	17.83	W_g	21.43

The simulation results depicted in Fig 11 show that the bandwidth is comparable with the smaller values of the first proposed antenna. However the major benefit is the compactness of the antenna. It has much reduced size.

3. SIMULATION AND MEASUREMENT RESULTS OF ANTENNAS

The antennas are fabricated and tested to validate the design and simulation results. The simulated and measured results of return loss for the first antenna are shown in Fig 8. From the results, it can be seen that the proposed antenna covers 569.9 MHz bandwidth from 1.66 GHz to 2.23 GHz. Hence, the proposed antenna can be used in this state in several wireless communication systems as LTE Bands 1,2,3,4,9,10,23,25, 33,34,35,36,37,39.

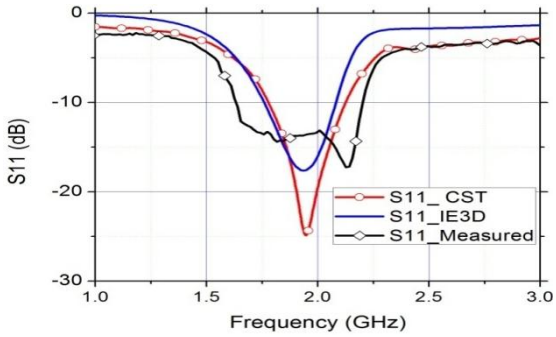

Fig 8: Comparison between the simulation and measured results for the first proposed antenna.

Radiation pattern of E plane and H plane at 1950 MHz can be seen in Fig 9. The 3D radiation pattern at 1950 MHz frequency can be seen in Fig 10. For the first proposed antenna. The radiation pattern is a characteristic of the patch antennas with directivity of 2.49 dBi.

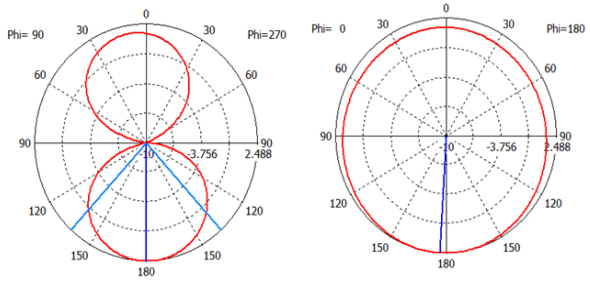

Fig 9: Radiation pattern of E plane and H plane at frequency 1950 MHz for the first proposed antenna.

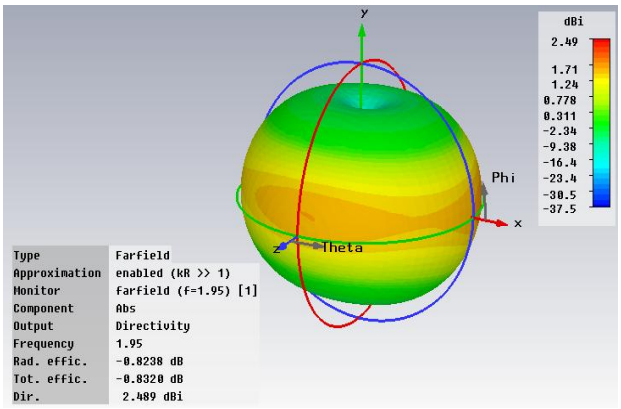

Fig 10: Simulated far-field 3D radiation pattern at frequency 1950 MHz for the first proposed antenna.

The simulated and measured results of return loss for the second antenna are shown in Fig 11. From the results, it can be seen that the proposed antenna covers 124.4 MHz bandwidth from 1.89 GHz to 2.017 GHz.

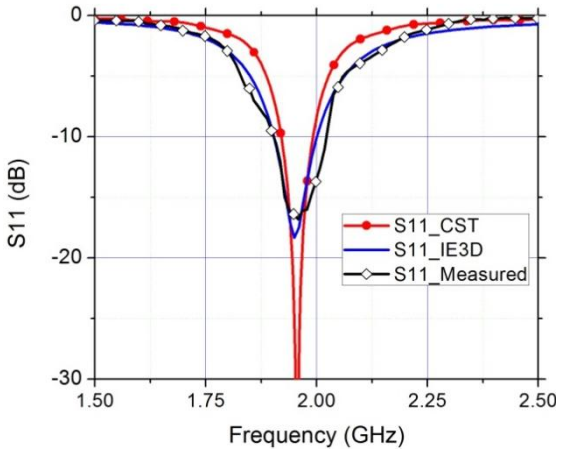

Fig 11: Comparison between the simulation and measured results for the second proposed antenna.

Radiation pattern of E plane and H plane at frequency 1950 MHz can be seen in Fig 12. The 3D radiation pattern at 1950 MHz frequency can be seen in Fig 13. For the second proposed antenna.

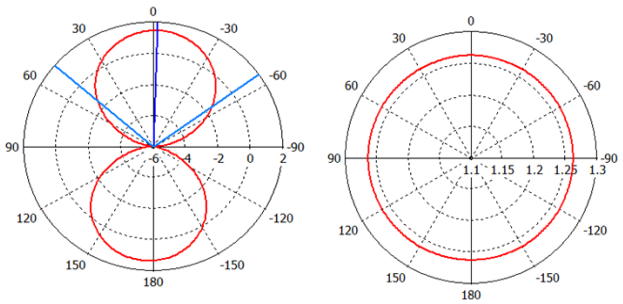

Fig 12: Radiation pattern of E plane and H plane at frequency 1950 MHz for the second proposed antenna.

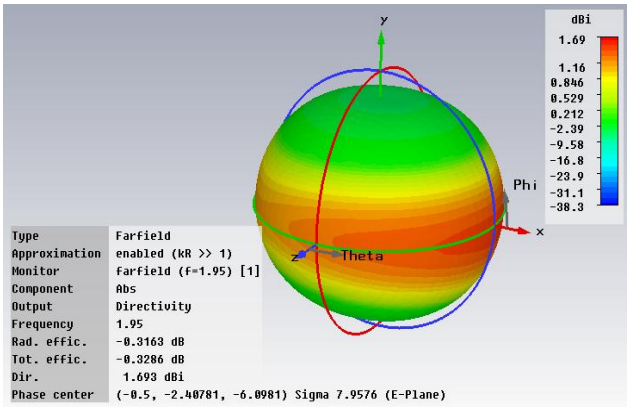

Fig 13: Simulated far-field 3D radiation pattern at frequency 1950 MHz for the second proposed antenna.

The radiation pattern is again a characteristic of the patch antennas with a directivity of 1.69 dBi. This antenna is fewer directives and has greater radiation efficiency than the first antenna.

4. BASICS OF FILTER

4.1. Transfer Function

In Radio Frequency (RF) applications, for defining transfer function we use the scattering parameter S21. In many applications we use instead the magnitude of S21, the quadratic of S21 is preferred

$$|S_{21}(j\Omega)|^2 = \frac{1}{1+\varepsilon^2 F^2(\Omega)} \quad (6)$$

ε is the ripple constant, $F_n(\Omega)$ filter function and Ω is frequency variable. If the transfer function is given [10], the insertion loss response of the filter can calculated by

$$L_A(\Omega) = 10\log\frac{1}{|S_{21}(j\Omega)|^2}\,dB \quad (7)$$

For lossless conditions, the return loss can be found by

$$L_R(\Omega) = 10\log[1 - |S_{21}(j\Omega)|^2]dB \quad (8)$$

4.2. Chebyshev Filter

In practical implementation, the specification for losses in pass region can normally be higher than zero. Chebyshev approach exploits this not so strictly given specification values. It can be 0.01 dB, or 0.1 dB, or even higher values. The Chebyshev approach thereby shows certain ripples in the pass region, this can lead to better (higher) slope in the stop region [5]. Fig 14 shows the attenuation characteristics for lowpass filter based on Chebyshev approach.

The quadrate of the magnitude of the transfer function with Chebyshev approach is given by

$$|S_{21}(j\Omega)|^2 = \frac{1}{1+\varepsilon^2 T_n{}^2(\Omega)} \quad (9)$$

$T_n(\Omega)$ is Chebyshev function type 1 with order n.

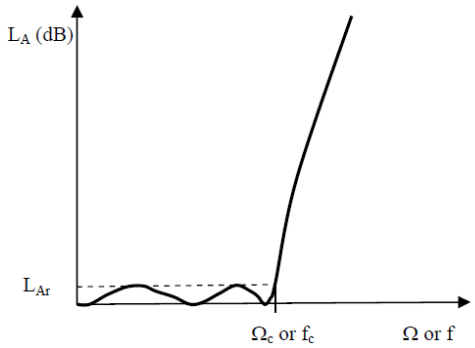

Fig 14: Attenuation characteristics for Chebyshev approach.

The normalized component values of the LC ladder network shown in Fig 15 and representing the prototype low pass filter with order n can be calculated from the following [10] rules:

$$g_0 = 1 \quad (10)$$

$$g_1 = \frac{1}{\gamma}\sin\left(\frac{\pi}{2n}\right) \quad (11)$$

$$g_i = \frac{1}{g_{i-1}} \frac{4\sin\left(\frac{\pi(2i-1)}{2n}\right)\sin\left(\frac{\pi(2i-3)}{2n}\right)}{\gamma^2+\sin^2\left(\frac{\pi(2i-1)}{n}\right)} \quad \text{for } i = 2 \text{ to } n \quad (12)$$

$$g_{n+1} = \begin{cases} 1 & n \text{ odd} \\ \coth^2\left(\frac{\beta}{4}\right) & n \text{ even} \end{cases} \quad (13)$$

Where

$$\beta = \ln\left(\coth\left(\frac{L_{Ar}}{17.37}\right)\right) \quad \text{And} \quad \gamma = \sinh\left(\frac{\beta}{2n}\right)$$

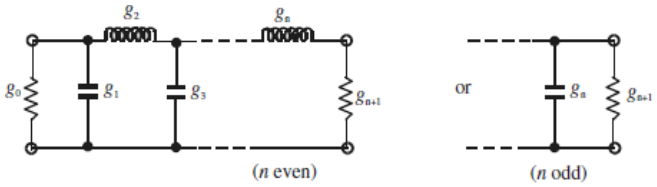

Fig 15: Lowpass prototype filters for all-pole filters with a ladder network structure

4.3. Transformation to Bandpass Filter

A transformation to bandpass is needed for getting bandpass characteristics. In the transformation, the component L will be converted to serial combinations of L_S and C_S, whereas the component C becomes parallel combination of L_P and C_P. With the cut-off frequencies ω_1 and ω_2 as lower and upper boundary [5, 10], we can calculate the center frequency and the relative frequency bandwidth as follows

$$\omega o = \sqrt{\omega 1 \omega 2} \quad \text{and} \quad FBW = \frac{\omega 2 - \omega 1}{\omega o}$$

And the values for the new components are

$$L_S = \left(\frac{1}{FBW.\omega o}\right) Zo.\, g \quad (14)$$

$$C_S = \left(\frac{FBW}{\omega o}\right)\frac{1}{Zo.g} \quad (15)$$

For the series combination, and

$$C_P = \left(\frac{1}{FBW.\omega o}\right)\frac{g}{Zo} \quad (16)$$

$$L_P = \left(\frac{FBW}{\omega o}\right)\frac{Zo}{g} \quad (17)$$

for the parallel combination.

Z_o is the value of the load impedance, normally set to 50 Ω.

4.4. Filter Realization with Microstrip Technology

Microstrip transmission line is the most used planar transmission line in Radio frequency (RF) applications [7]. The planar configuration can be achieved by several ways, for example with the photolithography process or thin-film and thick film technology. As other transmission line in RF applications, microstrip can also be exploited for designing certain components, like filter, coupler, transformer or power divider.

Coupled microstrip lines are widely used for implementing microstrip filters. Fig. 16 illustrates the cross section of a pair of coupled microstrip lines, where the two microstrip lines, of width W, are in parallel coupled configuration with a separation S. This coupled line structure supports two quasi-TEM modes, the even mode and the odd mode [5,10].

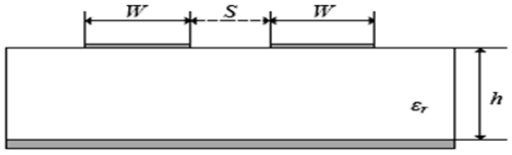

Fig 16: Cross section of coupled microstrip lines.

4.5. Designing Bandpass Filter

Fig 17 illustrates a general structure of parallel-coupled (or edge-coupled) microstrip bandpass filters that use half-wavelength line resonators [5]. They are positioned so that adjacent resonators are parallel to each other along half of their length. This parallel arrangement gives relatively large coupling for a given spacing between resonators, and thus,

this filter structure is particularly convenient for constructing filters having a wider bandwidth as compared to the structure for the end coupled microstrip filters. The design equations for this type of filter are given by [10]:

$$J_{01}Z_o = \sqrt{\frac{\pi}{2}\frac{FBW}{g_0 g_1}} \quad (18)$$

$$J_{j,j+1}Z_o = \frac{\pi FBW}{2}\frac{1}{\sqrt{g_{n-1}g_n}} \quad \text{For} \quad j = 1 \text{ to } n-1 \quad (19)$$

$$J_{n,n+1}Z_o = \sqrt{\frac{\pi}{2}\frac{FBW}{g_n g_{n+1}}} \quad (20)$$

Where g_0, g_1,……..g_n are the elements of a ladder-type lowpass prototype with a normalized cutoff $\omega_c = 1$ rad/sec, and FBW is the fractional bandwidth of bandpass filter, $J_{n,n+1}$ are the characteristic admittances of J-inverters and Y_0 is the characteristic admittance of the terminating lines.

We can calculate the characteristic impedances of even-mode and odd-mode of the parallel-coupled microstrip transmission line, as follows

$$(Z_{0e})_{j,j+1} = \frac{1}{Yo}\left[1 + \frac{Jj,j+1}{Yo} + \left(\frac{Jj,j+1}{Yo}\right)^2\right] \quad (21)$$

For j = 0 to n, and

$$(Z_{0o})_{j,j+1} = \frac{1}{Yo}\left[1 - \frac{Jj,j+1}{Yo} + \left(\frac{Jj,j+1}{Yo}\right)^2\right] \quad (22)$$

For j = 0 to n.

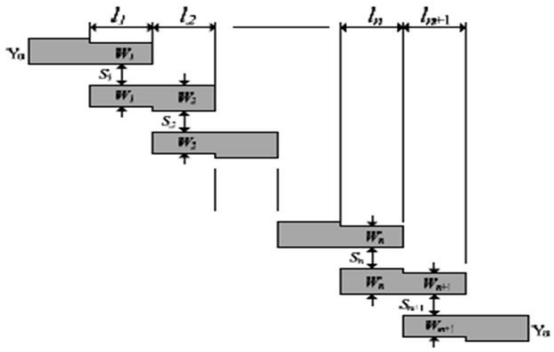

Fig 17: General Structure of parallel (edge)-coupled microstrip bandpass filters.

Now, a narrow band bandpass filter based on a conventional parallel coupled-line structure is designed. The response of coupled-line filter exhibits sufficient bandwidth that covers LTE bands 1 or 36 (1920-1980MHz) application as base station BPF but its undesired passband must be minimized.

The target specifications of BPF are as a following:

- Center frequency = 1.95 GHz
- 3 dB bandwidth =80 MHz (FBW = 4.01%)
- |S21| better than -3 dB
- |S11| less than -20 dB
- The ripple factor in the passband is 0.01 dB.
- Characteristic impedance = 50 Ω

The substrate material is FR4 with dielectric constant ε_r=4.5, dielectric thickness h=1.6 mm, and loss tangent tan δ =0.025. A Chebyshev prototype with 0.01 dB ripple is used in the design. For third order prototype filter n = 3, the parameters are

$g_0 = g_4 = 1$

$g_1 = g_3 = 0.6292$

$g_2 = 0.9703$

$$\frac{J_{01}}{Y_0} = \sqrt{\frac{\pi}{2}\frac{FBW}{g_0 g_1}} = 0.32 = \frac{J_{34}}{Y_0}$$

$$\frac{J_{12}}{Y_0} = \frac{\pi FBW}{2}\frac{1}{\sqrt{g_1 g_2}} = 0.0824 = \frac{J_{23}}{Y_0}$$

Then we calculate the even-mode and odd-mode characteristic impedances of this parallel coupled

microstrip line using eq. (21) and (22), which leads to

$(Z_{0e})_{01} = 71.12\ \Omega = (Z_{0e})_{34}$

$(Z_{0o})_{01} = 39.12\ \Omega = (Z_{0o})_{34}$

$(Z_{0e})_{12} = 56.46\ \Omega = (Z_{0e})_{23}$

$(Z_{0o})_{12} = 46.22\ \Omega = (Z_{0o})_{23}$

With the procedure explained in [5, 10, 11], we can determine the width of parallel-coupled microstrip lines W and the distance between them s.

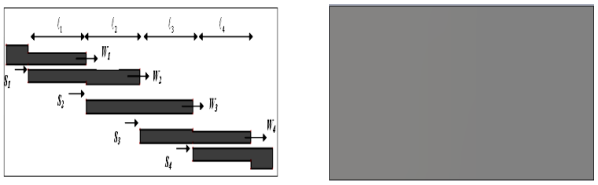

(a) (b)

Fig 18: The geometry of the conventional parallel coupled-line BPF without DGS. (a) Top view (b) Bottom view.

Table 4: Geometric dimensions of the conventional parallel coupled-line BPF.

N	W_n (mm)	S_n (mm)	l_n (mm)
1 and 4	1.38	0.8	19.671
2 and 3	2.1911	1.407	19.648

The overall dimension 84.4*21.8mm

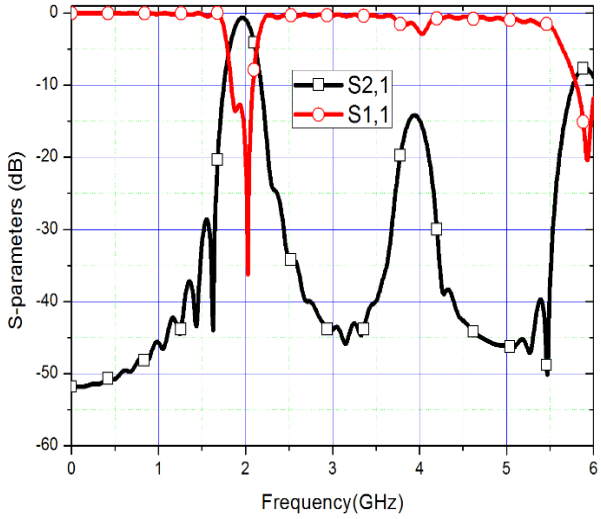

Fig 19: the simulated reflection and transmission coefficients of the conventional parallel coupled-line BPF without DGS.

The simulated response of parallel coupled-line BPF is shown in Fig 19. The filter has 3 dB bandwidth from 1.91:2.00 GHz. By inspecting the results, it is clear that the parallel coupled-line BPF consumes relatively large area with overall dimensions of 84.4mm * 21.8mm, which means it is bulky. So, design the parallel coupled-line BPF with DGS to enhance this conventional type.

4.6.Parallel Coupled-line BPF with DGS

The configuration of the parallel coupled-line BPF with DGS [6] is illustrated in Fig. 20.The filter was designed on FR4 epoxy substrate with the overall dimension of 45*25 mm^2. The Performance of a Band pass Filter Enhancement by DGS and the passband center frequency is 1.95 GHz with -3dB bandwidth of 80 MHz (4.1%). It is observed also that the attenuation of the second and third harmonics around 3.9 GHz and 5.9 GHz respectively, are well below -28 dB and the stopband extends up to 6 GHz and offers a sharpness factor of 74dB/GHz and the filter size reduces to 45mm*25mm

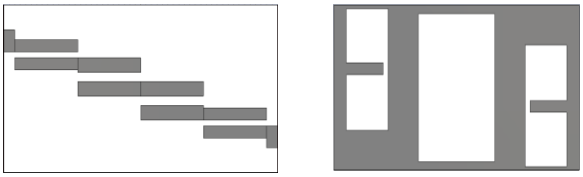

(a) (b)

Fig 20: The geometry parallel coupled-line BPF with DGSs. (a) Top view (b) Bottom view.

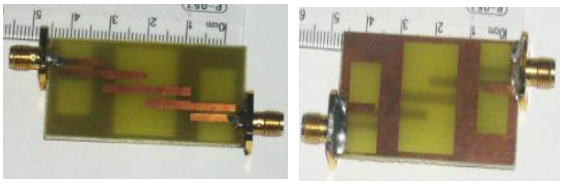

(a) (b)

Fig 21: A photo of fabricated three-pole parallel coupled-line BPF with DGSs. (a) Top view. (b) Bottom view.

Table 5: Geometric dimensions of the parallel coupled-line BPF with DGS.

N	W_n (mm)	S_n (mm)	l_n (mm)
1 and 4	1.78	0.9	11.55
2 and 3	2.1911	1.36	11.45

The overall dimensions 45*25mm

5. SIMULATION AND MEASUREMENT RESULTS OF BPF

The fabricated filter is shown in the photo of Fig. 21.The simulation results of the parallel coupled BPF with and without DGS is shown in fig. 22.

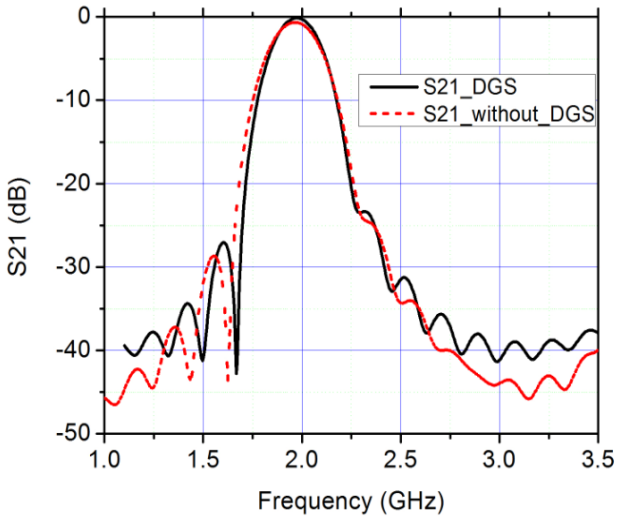

Fig 22: shows the simulation results the parallel couple BPF with and without DGS.

The simulation and measured results of BPF with DGS is shown in fig 23.

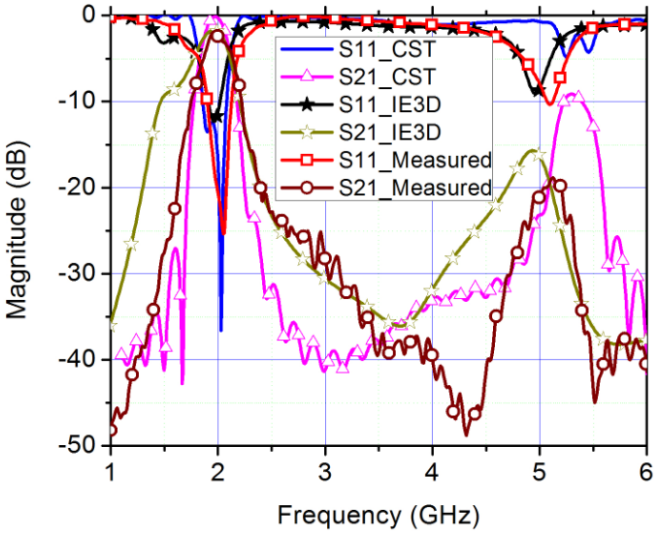

Fig 23: The simulated and measured reflection and transmission coefficients of the parallel coupled-line BPF with DGS.

Fig 23 shows the simulated and measured S-parameters for the filter. It is found slight Performance Enhancement of a Band pass Filter by DGS and the passband center frequency is 1.95 GHz with -3dB bandwidth of 80 MHz (4.1%). The major advantage of the DGS is that the filter size reduces to 45mm*25mm.

6. CONCLUSION

The proposed two antennas and filter are used for LTE system. The antennas and filter are fabricated on FR4 substrate which is a low cost. Firstly the size of the proposed antennas is smaller than the conventional patch antenna because of the partial ground. The size of the first antenna design reduced by 22% while the size of the second antenna design fell by greater than 50% compared to the size of conventional patch antenna. The bandwidth of the first and second proposed antenna is 0.57 GHz (1.666 - 2.2395 GHz) and 0.127 GHz (1.89 - 2.017 GHz) respectively. The first antenna has a gain and directivity of 1.7dB and 2.5 dBi with omnidirectional radiation pattern. The second antenna has a gain and directivity of 1.4 dB and 1.7 dBi with omnidirectional radiation pattern.

Secondly the proposed filter is a third order parallel couple filter with defected ground structure. With DGS the dimension of filter reduced from 84.4 mm*21.8 mm to 45 mm* 25 mm and the filter became more sharpness. The DGS band pass filter operates at center frequency 1.95 GHz and 3 dB frequency 80 MHz.

In the future work we shall implement a complete RF front end including PA, Mixers and frequency synthesizer.

7. REFERENCES

[1] 3GPP TS 36.101, V8.3.0, "EUTRA User Equipment Radio Transmission and Reception," September 2008.

[2] C. A. Balanis, Antenna theory, 3rd edition, John Wiley, New York, 2005.

[3] C. C. Chiaw, "Novel design of circular and monopole UWB antenna," MSc. Thesis, Universiti Teknologi Malaysia, 2009.

[4] C.-H. Ku, H.-W. Liu, and Y.-X. Ding, "Design of planar coupled-fed monopole antenna for eight-band

LTE/WWAN mobile handset application," Progress In Electromagnetics Research C, Vol. 33, pp. 185-198, 2012

[5] J.S. Hong and M.J. Lancaster, ''Microstrip Filters for RF/Microwave Applications,'' John Wiley & Sons, 2011.

[6] J. S. Yun, J. S. Park, D. Ahn, "A design of the novel coupled-line bandpass filter using defected ground structure with wide stopband performance," IEEE Transaction on Microwave Theory and Techniques, Vol.50, No.9, pp.2037~2043, Sept. 2002.

[7] Mudrik Alaydrus," Designing Microstrip Bandpass Filter at 3.2 GHz", International Journal on Electrical Engineering and Informatics - Volume 2, Number 2, 2010.

[8] XuanxuanWang, WenxiuWang, DanShi, and YougangGao, "Design and Simulation of TD-LTE Dual-mode Mobile Terminal Antenna Combined with MIMO Technology," IEEE Antennas and Wireless Propag. Lett., vol. 12, pp. 46–49, 2011.

[9] Mandana Mehrparvar, Omid Hoseini Izadi, and Homayoon Oraizi, "Design of Microstrip Spiral Antenna Using Genetic Algorithm," IEEE 6th International Symposium on Telecommunications, vol. 12, pp. 11-14, 2012.

[10] D. M. Pozar, Microwave Engineering, Fourth Edition, Wiley and Sons, 2012.

[11] Reshma R. Lokapure And Hassanali Virani, ''Design of Parallel Coupled Microstrip bandpass Filter ,'' International Conference on Electronics and Communication Engineering, 28th April-2013.